Spin identification of Higgs boson in diphoton production at the Large hadron collider

18th International Seminar on High Energy Physics

QUARKS-2014

2-8 June, 2014 Suzdal, Russia,

***A.V. Tsytrinov*, A.A. Pankov**

The Abdus Salam ICTP Affiliated Centre @

Technical University of Gomel (Belarus)

with:

V.A. Bednyakov

JINR, Dubna

(Russia)

N. Paver

University of Trieste,

INFN-Sezione di Trieste (Italy)

Introduction

In 2012 the ATLAS and CMS Collaborations published the discovery of a new 126 GeV resonance **[Phys. Lett. B 716 (2012) 1, Phys. Lett. B 716 (2012) 30]** in the search for the Standard Model (SM) Higgs boson. The present experimental challenge is to compare its properties with the SM predictions for the Higgs boson. In the SM, the Higgs boson is a spin-0 and CP-even particle ($J^P = 0^+$). The Landau–Yang theorem forbids the direct decay of an on-shell spin-1 particle into a pair of photons [**Dokl. Akad. Nauk Ser. Fiz. 60 (1948) 207**, **Phys. Rev. 77 (1950) 242**]. The spin-1 hypothesis is therefore strongly disfavoured by the observation of the $H \rightarrow \gamma\gamma$ decay.

The CMS Collaboration has published a spin–parity study [**Phys. Rev. Lett. 110 (2013) 081803**] based on the $H \rightarrow ZZ$ channel where the SM scalar hypothesis is favoured over the pseudoscalar hypothesis at a confidence level (CL) above 95% .

The ATLAS Collaboration has published a spin–parity study **[Phys. Lett. B 726 (2013) 120]** where the $J^P = 0^+$ hypothesis of the SM was compared to several alternative hypotheses with $J^P = 0^-; 1^+; 1^-; 2^+$. The measurements were based on the kinematic properties of the three final states:

$$H \rightarrow \gamma\gamma,\ H \rightarrow ZZ^* \rightarrow 4\ell \text{ and } H \rightarrow WW^* \rightarrow \ell\nu\ell\nu,$$

and SM scalar hypothesis is favoured over others at 3-4 sigma level.

Introduction

- The measurement of the total number of events, the angular distribution dσ/dcosθ, and the center-edge asymmetry A_{CE} of photon decay products at the resonance peak is a powerful tool to disentangle the spin of the resonance observed, and hence to identify its spin in $p+p\rightarrow\gamma\gamma+X$

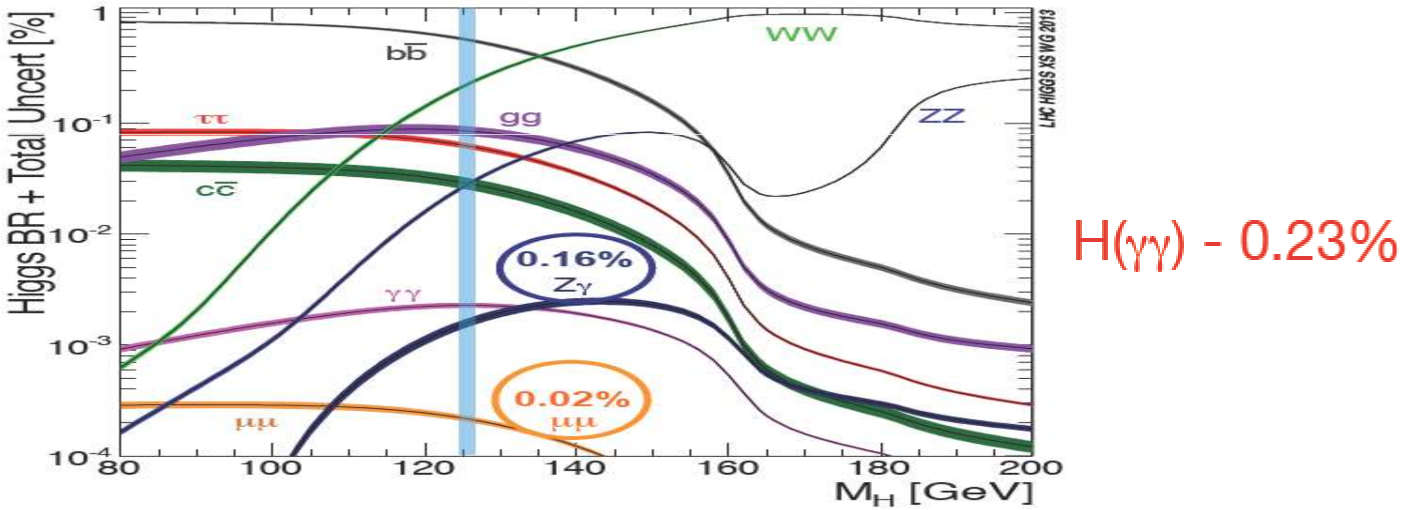

- The angular study is not considered here as it requires more integrated luminosity as the one available in the first phase of data taking at the LHC.

$$\boxed{p+p\to\gamma\gamma+X}$$

[*M.C. Kumar, P. Mathews, A.A. Pankov, N. Paver, V. Ravindran, A.V. Tsytrinov*
PHYSICAL REVIEW D 84, 115008 (2011)]

- $V \not\to \gamma\gamma$ excludes spin-1: $\dfrac{G\to\gamma\gamma}{G\to l^+l^-}\sim 2$ – <u>predicted</u> => strong test

Landau – Yang theorem
[Dokl.Akad.Nauk.SSSR, V.60, P.207 (1948); Phys.Rev. V.77, P.242 (1950)]

- Can identify the spin? ***A**$_{CE}$*–based analysis applicable. **[Phys.Rev. D78, 035008 (2008); Phys.Rev. D 84, 115008 (2011), Alves, Phys.Rev. D86 (2012) 113010]**

z = cosθ*

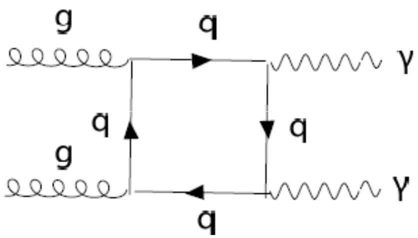

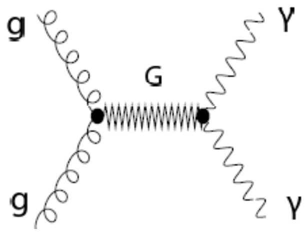

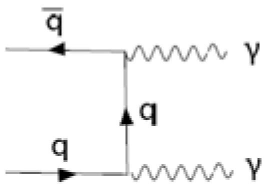

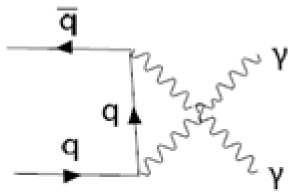

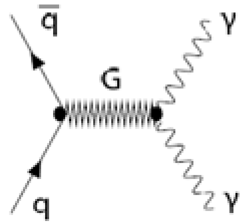

- $g\,g\to G\to\gamma\gamma \;\propto\; 1+6z^2+4z^4$: dominant, peaked at **z = ±1**
- $q\,\bar{q}\to G\to\gamma\gamma \;\propto\; 1-z^4$

NLO QCD effects for diphoton process:

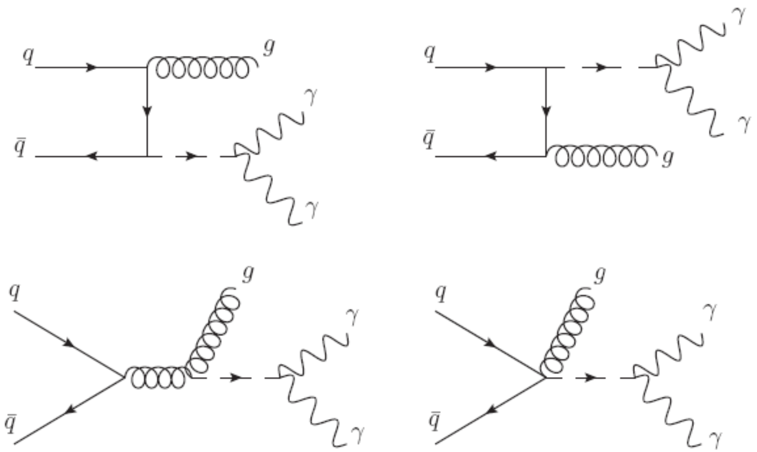

Feynman diagrams contributing to the subprocess qbarq → gγγ. The dashed line could be either R = G or S depending on the model. For the scalar exchange S the last diagram involving a four point vertex does not exist.

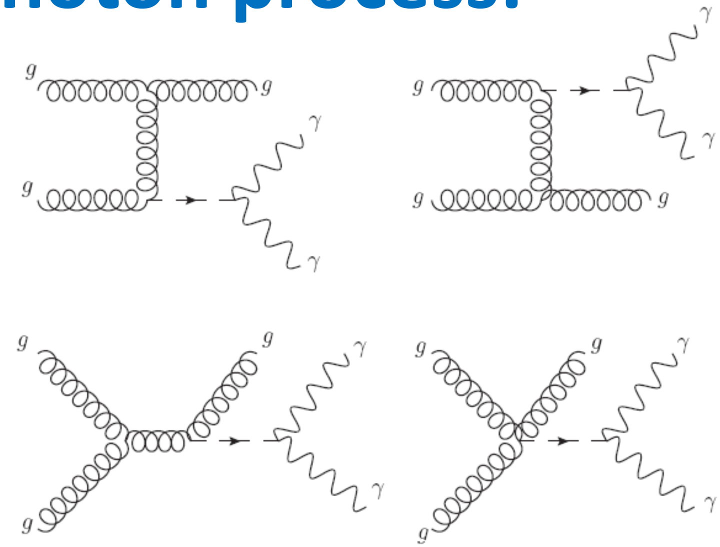

Feynman diagrams contributing to the subprocess gg → g γγ, where the dashed line corresponds to a spin-2 RS KK mode G or a scalar exchange S. In the case of a scalar exchange the last diagram involving a four point vertex does not exist.

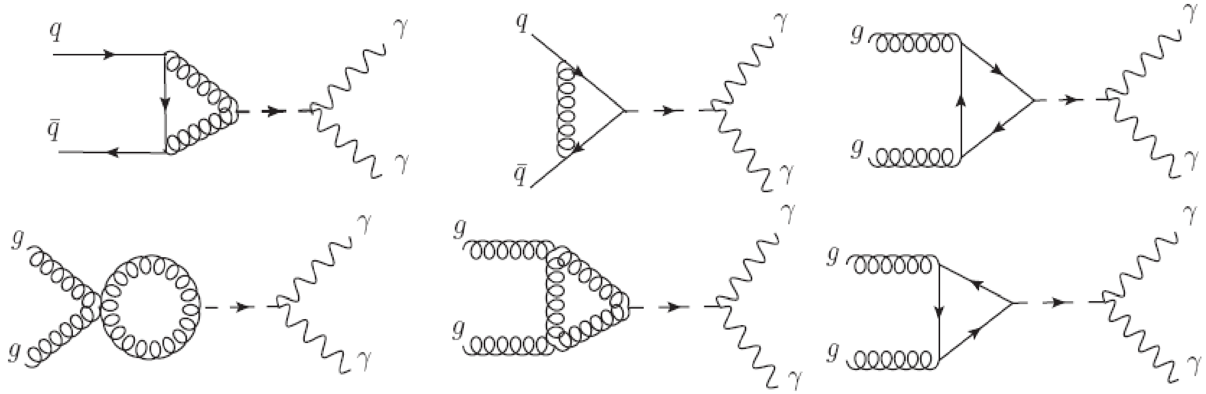

Feynman diagrams contributing to one loop subprocess to the qbarq and gg channel in the NP models.

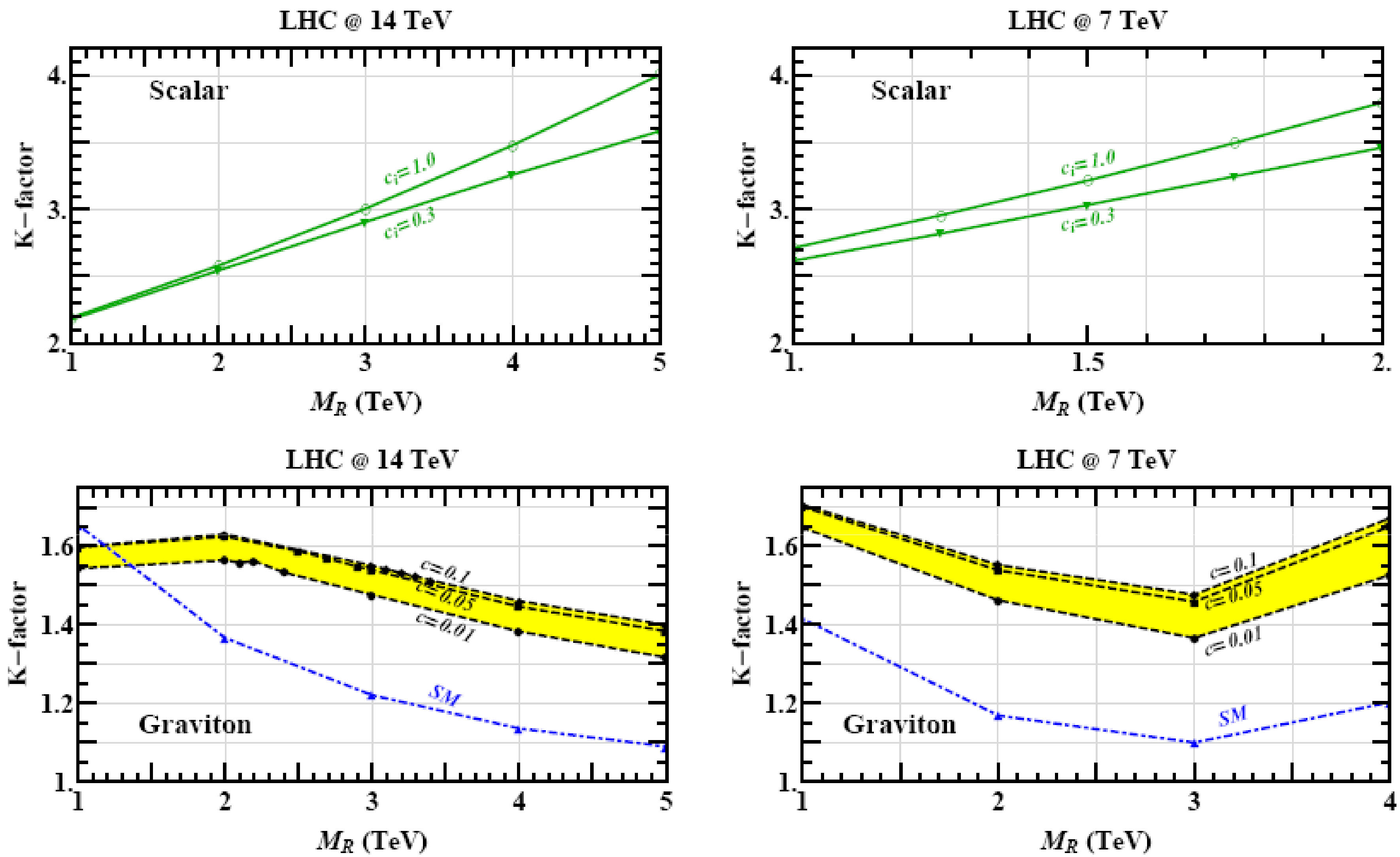

K-factor vs M_R for 14 TeV (left panel) and 7 TeV (right panel) LHC.

Experimental cuts: p > 40 GeV; |η| < 2.4; ε = 80%

K-factor *vs.* cosθ, 14 TeV LHC.

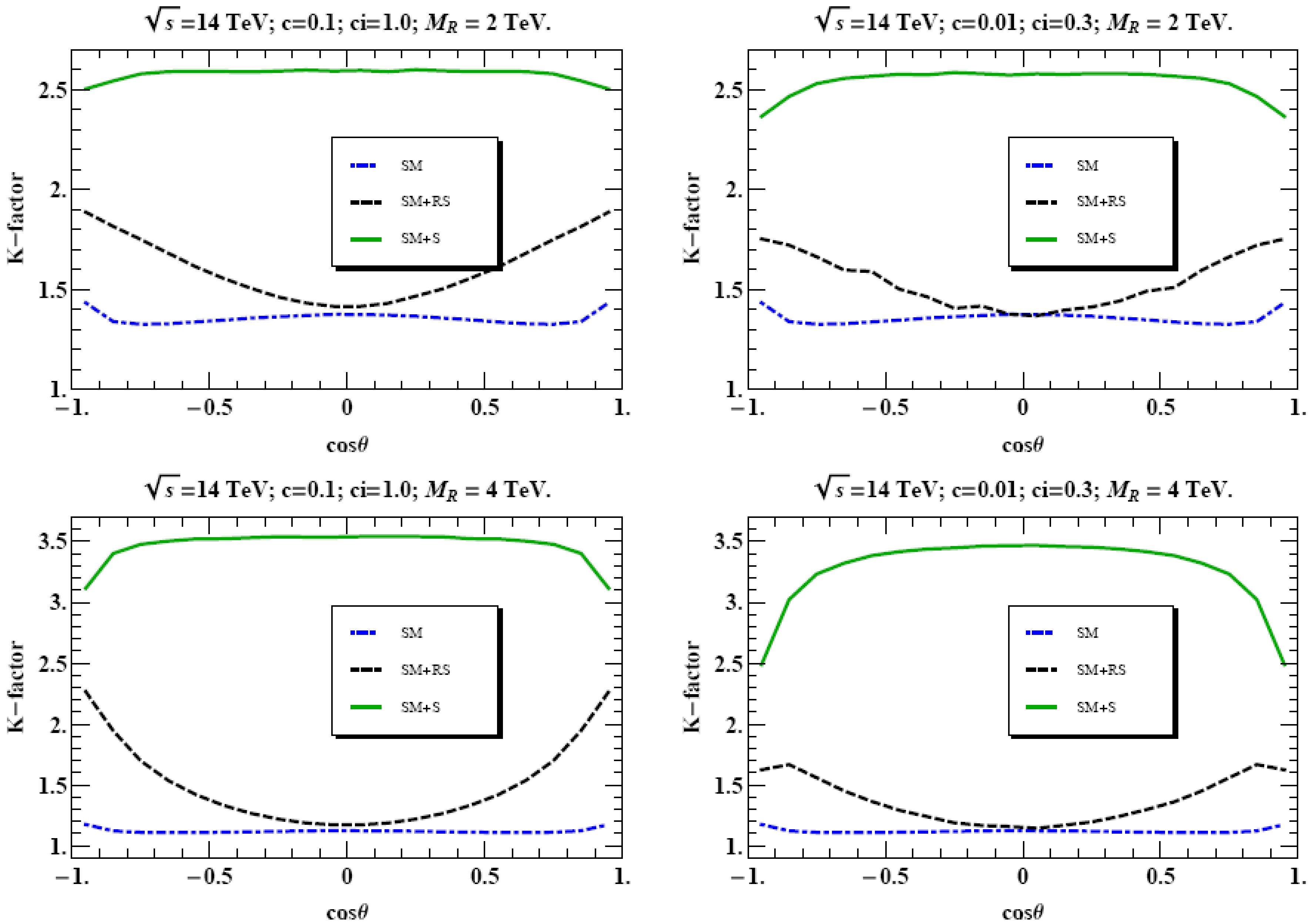

A_{CE} analysis

[Phys.Rev. D78, 035008 (2008); Phys.Rev. D 84, 115008 (2011)]

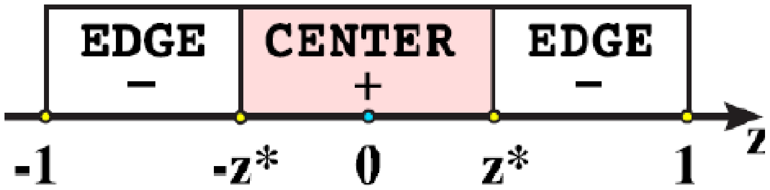

$$A_{\rm CE} = \frac{\sigma_{\rm CE}}{\sigma} \quad \text{with}$$

$$\sigma_{\rm CE} \equiv \left[\int_{-z^*}^{z^*} - \left(\int_{-z_{\rm cut}}^{-z^*} + \int_{z^*}^{z_{\rm cut}}\right)\right] \frac{{\rm d}\sigma}{{\rm d}z}\,{\rm d}z.$$

$$A_{CE}(spin2) = f_{qq} A_{CE}^{q\bar{q}} + (1 - f_{qq}) A_{CE}^{gg},$$

$$A_{CE} = \frac{\sigma_{CE}}{\sigma} = \frac{N_{CE}}{N}$$

$$N_{CE} = N_C - N_E$$

$$\delta A_{CE}^{data} = \frac{2N_E N_C}{(N_E N_C)^2}\sqrt{\frac{\sigma_C^2}{N_C^2} + \frac{\sigma_E^2}{N_E^2}}, \qquad \sigma_C^2 = \sum_{i=1}^{i_{z*}} \sigma_i^2, \qquad \sigma_E^2 = \sum_{i=i_{z*}}^{i_{z_{cut}}} \sigma_i^2,$$

Calculated from CERN-PH-EP-2013-102: Fig.2a

$$A_{CE}^{data} = 0.3247 \pm 0.1955.$$

LO and NLO A_{CE} asymmetry *vs.* z^* for the process $pp \to \gamma\gamma + X$ at 14 TeV LHC

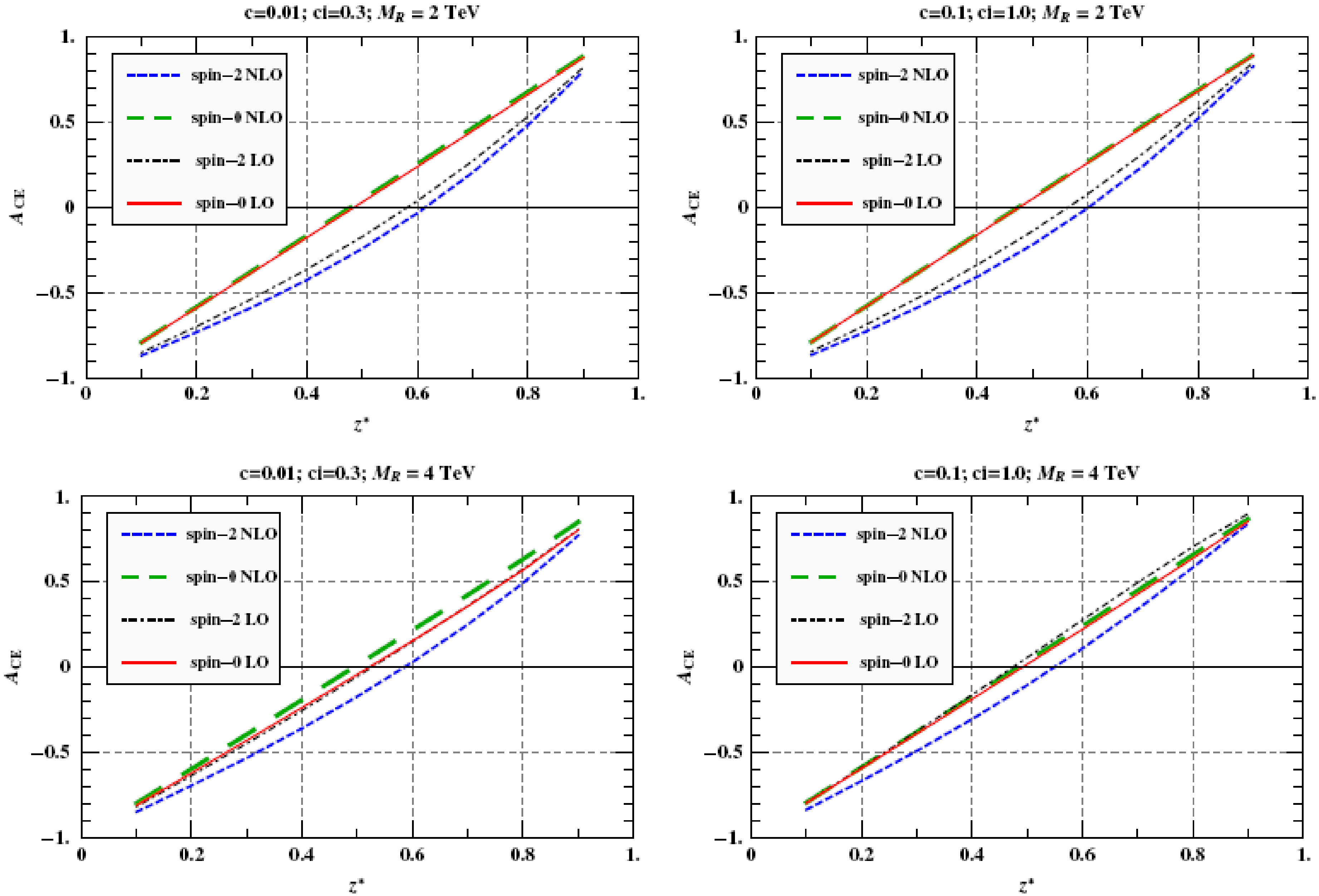

ATLAS recent data and simulations for pp →γγ +X

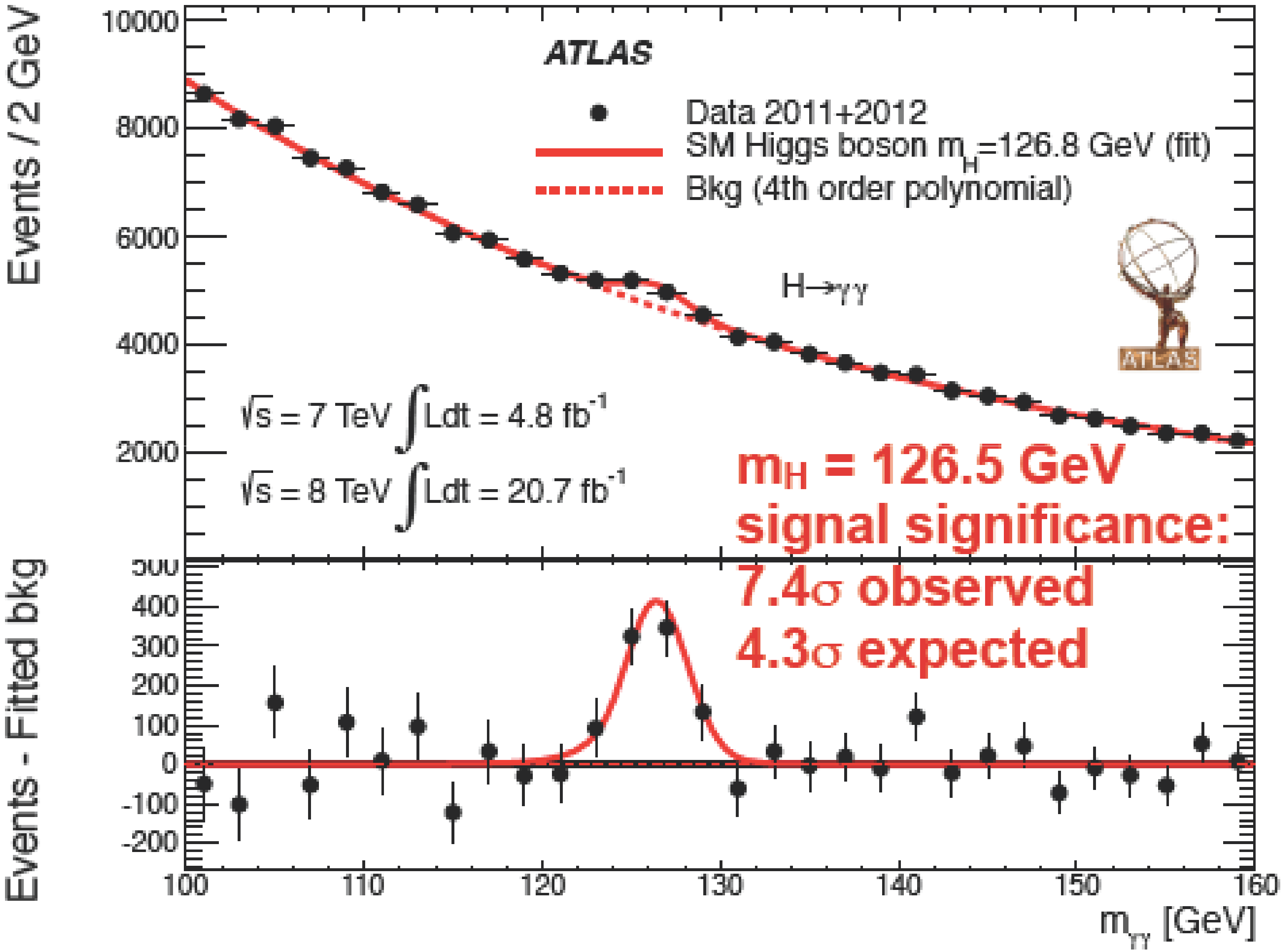

ATLAS recent data and simulations for pp →γγ +X

CERN-PH-EP-2013-102: Fig.1

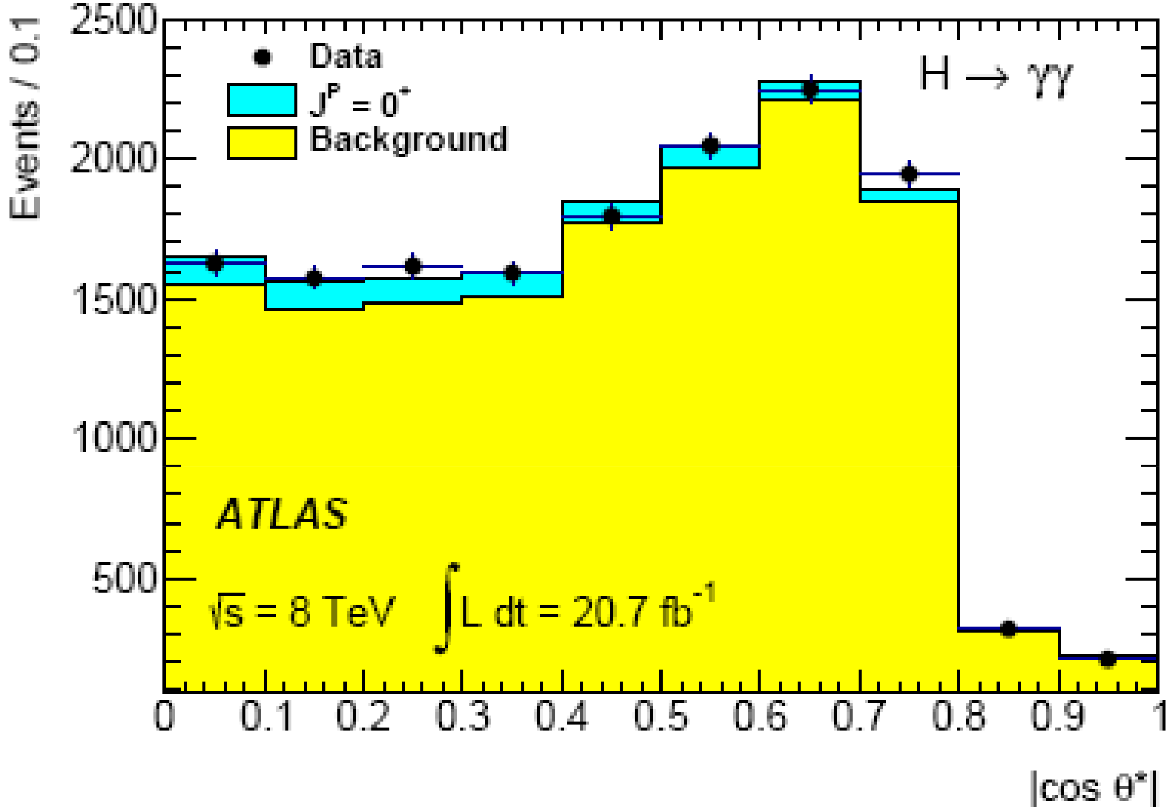

Figure 1: Distribution of $|\cos\theta^*|$ for events in the signal region defined by 122 GeV $< m_{\gamma\gamma} <$ 130 GeV. The data (dots) are overlaid with the projection of the signal (blue/dark band) and background (yellow/light histogram) components obtained from the inclusive fit of the data under the spin-0 hypothesis.

ATLAS recent data and simulations for pp →γγ +X

Theoretical predictions

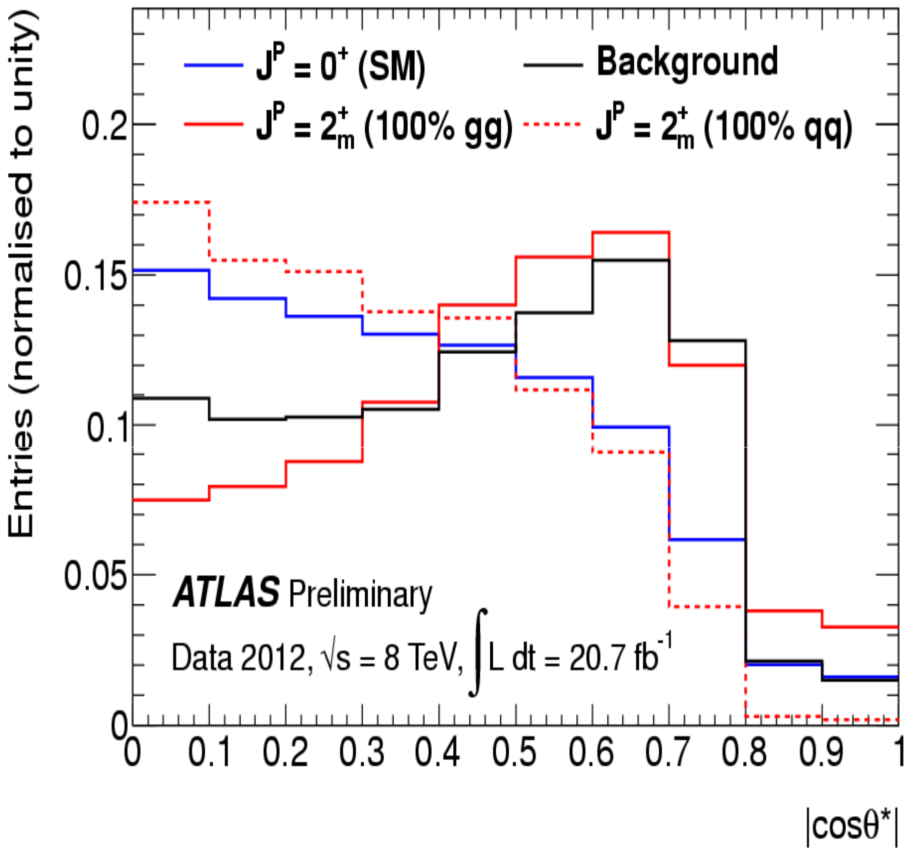

ATLAS-CONF-2013-029: Fig.5

ATLAS data (8 TeV)

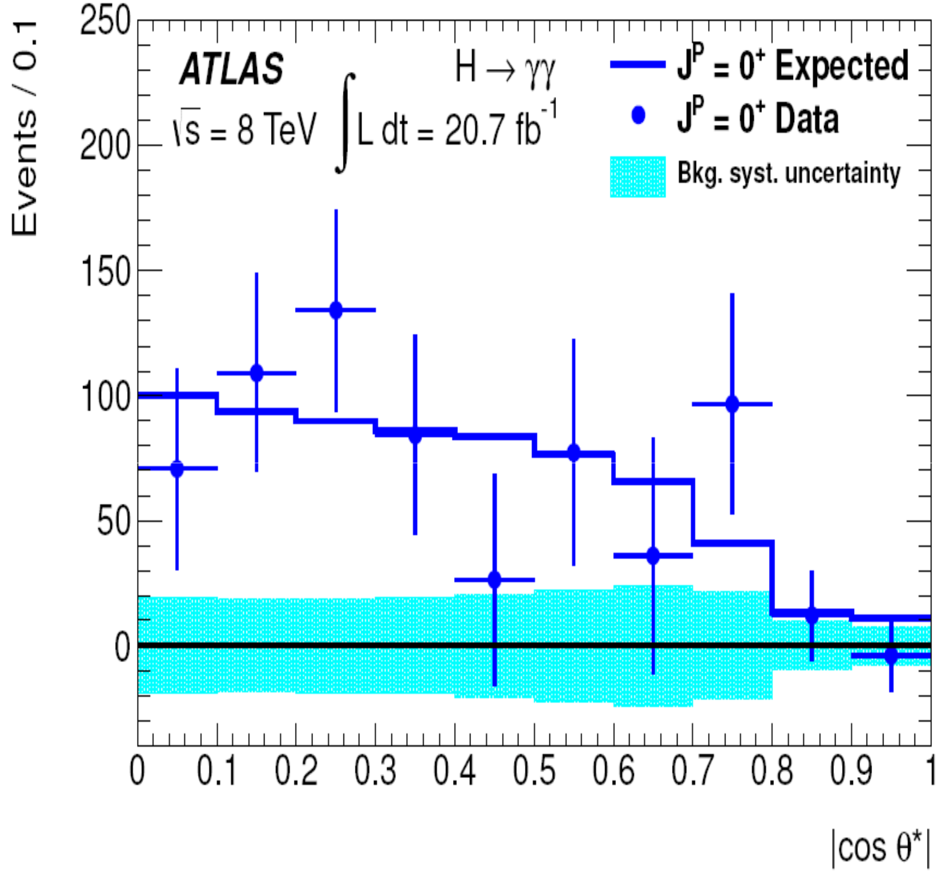

CERN-PH-EP-2013-102: Fig.2a

CERN-PH-EP-2013-102: Fig.8

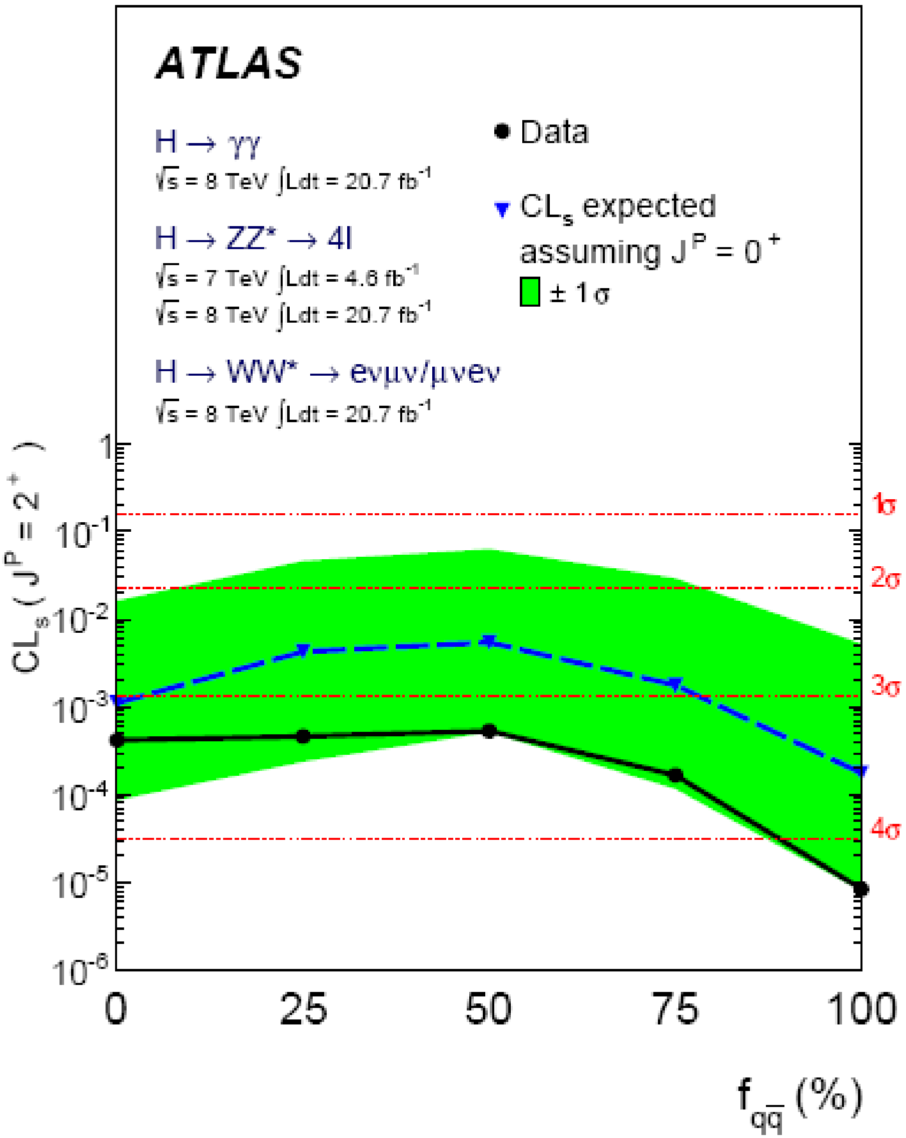

Figure 8: Expected (blue triangles/dashed line) and observed (black circles/solid line) confidence levels, $\mathrm{CL_s}(J^P = 2^+)$, of the $J^P = 2^+$ hypothesis as a function of the fraction $f_{q\bar{q}}$ (see text) for the spin-2 particle. The green bands represent the 68% expected exclusion range for a signal with assumed $J^P = 0^+$. On the right y-axis, the corresponding numbers of Gaussian standard deviations are given, using the one-sided convention.

The exclusion of the alternative J^P_{alt} hypothesis in favour of the Standard Model 0^+ hypothesis is evaluated in terms of the corresponding $\mathrm{CL_s}(J^P_{\mathrm{alt}})$, defined as:

$$\mathrm{CL_s}(J^P_{\mathrm{alt}}) = \frac{p_0(J^P_{\mathrm{alt}})}{1 - p_0(0^+)} .$$

$$N = f_{qq} N_{qq} + (1 - f_{qq}) N_{gg}$$

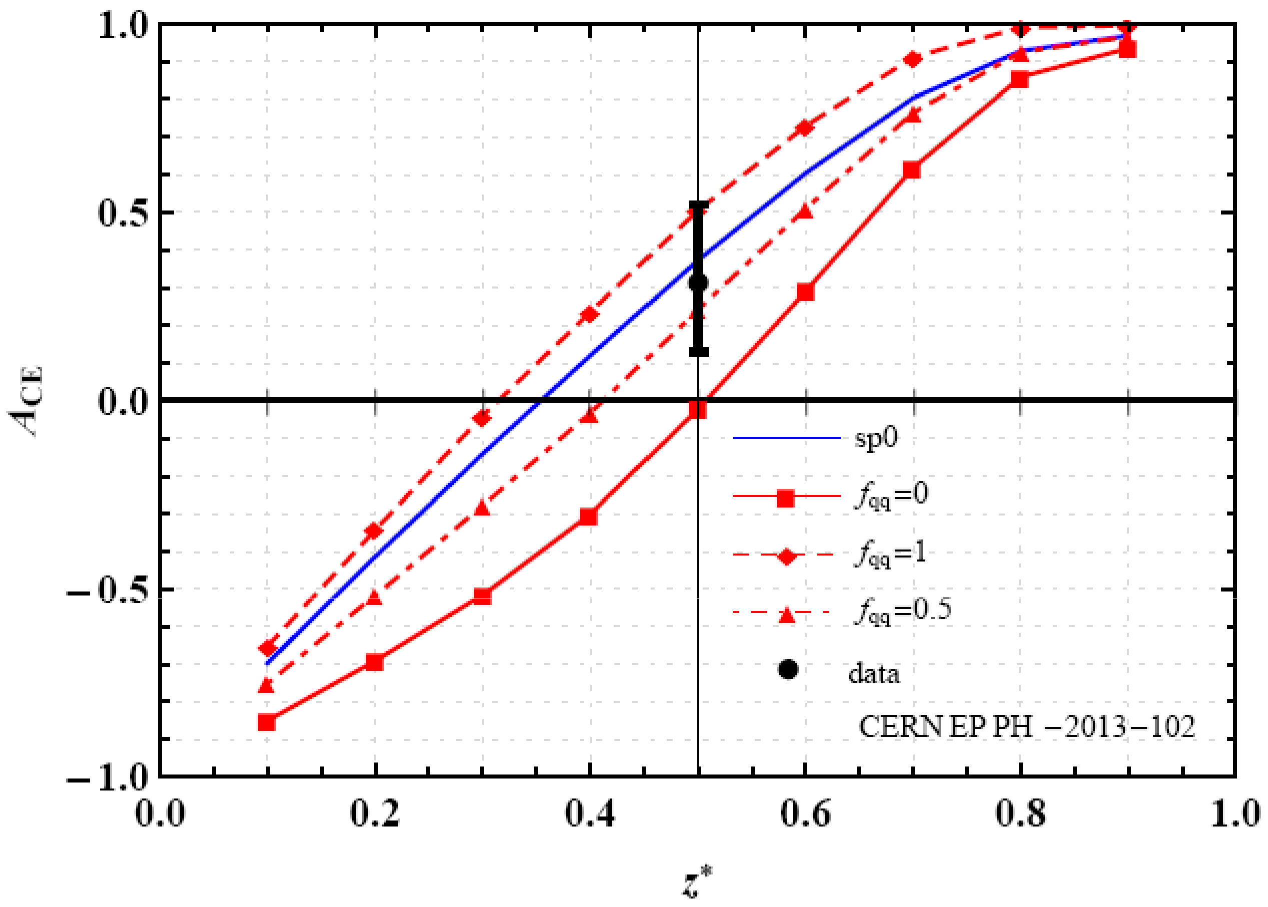

Figure 1: A_{CE} vs. z^* at the LHC in process (1) at $\sqrt{s}$ =8 TeV, $\mathcal{L}_{\rm int}$ = 20 fb^{-1}. A_{CE}^{data} = 0.3247 ± 0.1955 for z^*=0.5 is also presented.

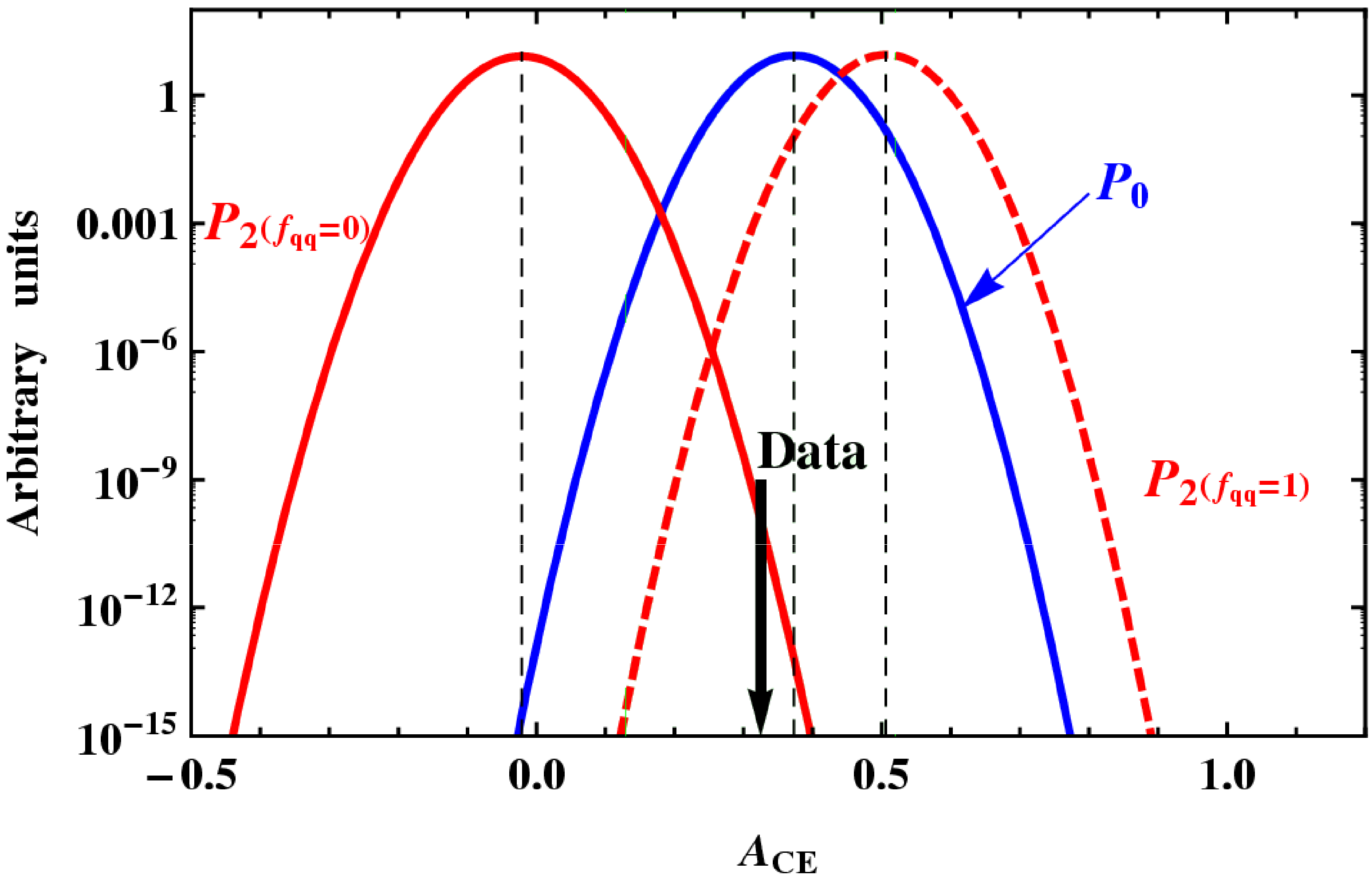

Figure 2: The probability density functions of the center-edge asymmetry A for spin-0 and spin-2 distributions. The data shown as an arrow.

The exclusion of the alternative J^P_{alt} hypothesis in favour of the Standard Model 0^+ hypothesis is evaluated in terms of the corresponding $\mathrm{CL_s}(J^P_{\mathrm{alt}})$, defined as:

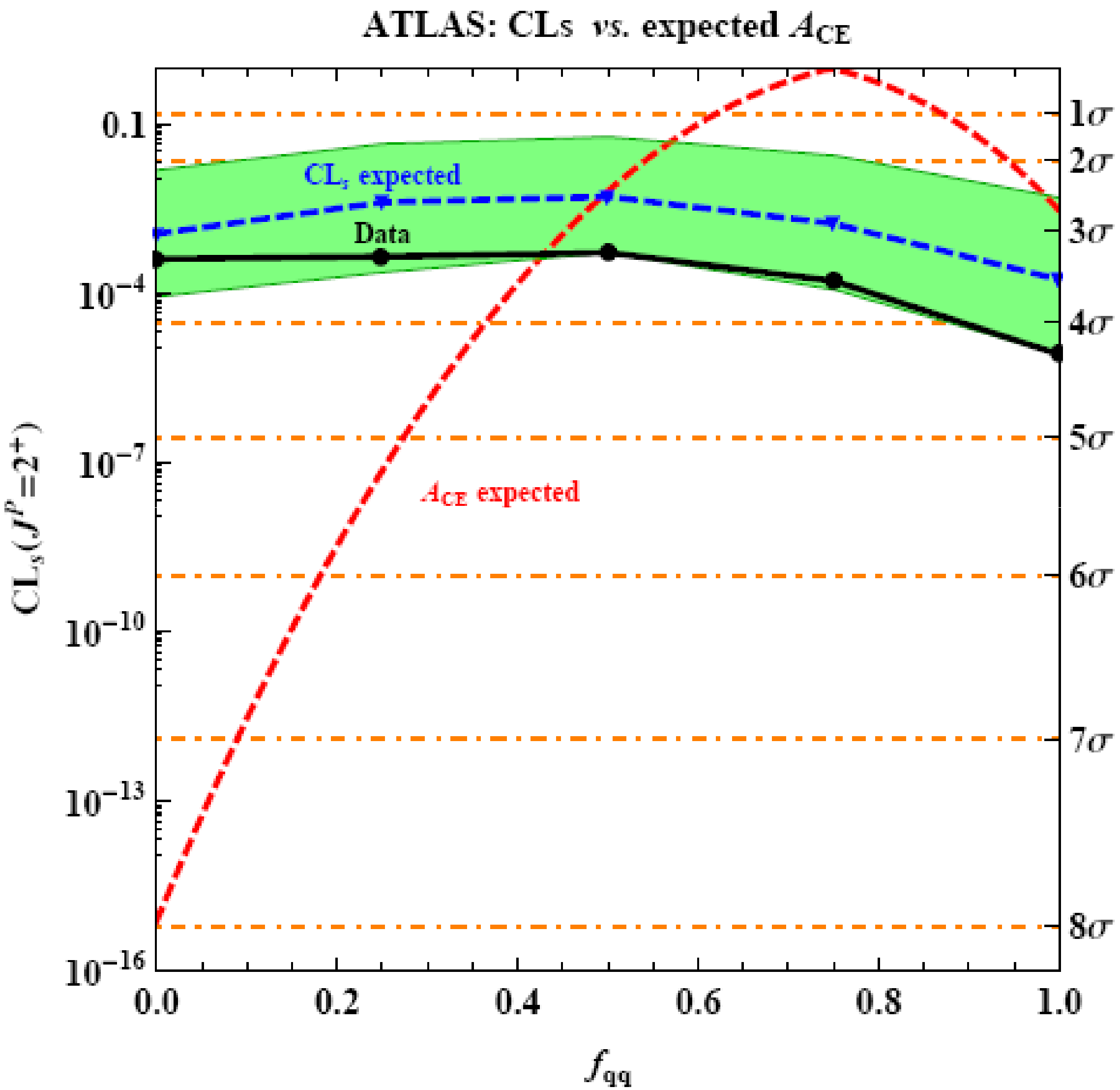

$$\mathrm{CL_s}(J^P_{\mathrm{alt}}) = \frac{p_0(J^P_{\mathrm{alt}})}{1 - p_0(0^+)} .$$

$$N = f_{qq} N_{qq} + (1 - f_{qq}) N_{gg}$$

Conclusions

1) We show that A_{CE} has a good potential to discriminate the hypotheses of resonances with spin-0 and spin-2 in particular in the parameter region of $0 < f_{qq} < 0.4$;

2) To perform more sophisticated analysis outlined above one needs current ATLAS data on di-photon angular distributions at 8 TeV for direct evaluation of A_{CE}.